
This is an electronic reprint of the original article.
This reprint may differ from the original in pagination and typographic detail.

Kastinen, Tuuva; Batys, Piotr; Tolmachev, Dmitry; Laasonen, Kari; Sammalkorpi, Maria
Ion-Specific Effects on Ion and Polyelectrolyte Solvation

Published in:
ChemPhysChem

DOI:
[10.1002/cphc.202400244](https://doi.org/10.1002/cphc.202400244)

Published: 01/08/2024

Document Version
Publisher's PDF, also known as Version of record

Published under the following license:
CC BY

Please cite the original version:
Kastinen, T., Batys, P., Tolmachev, D., Laasonen, K., & Sammalkorpi, M. (2024). Ion-Specific Effects on Ion and Polyelectrolyte Solvation. *ChemPhysChem*, 25(15), Article e202400244.
<https://doi.org/10.1002/cphc.202400244>

This material is protected by copyright and other intellectual property rights, and duplication or sale of all or part of any of the repository collections is not permitted, except that material may be duplicated by you for your research use or educational purposes in electronic or print form. You must obtain permission for any other use. Electronic or print copies may not be offered, whether for sale or otherwise to anyone who is not an authorised user.

Ion-Specific Effects on Ion and Polyelectrolyte Solvation

Tuuva Kastinen,^[a, b, c] Piotr Batys,^[d] Dmitry Tolmachev,^[a, b] Kari Laasonen,^[a] and Maria Sammalkorpi^{*[a, b, e]}

Ion-specific effects on aqueous solvation of monovalent counter ions, Na⁺, K⁺, Cl⁻, and Br⁻, and two model polyelectrolytes (PEs), poly(styrene sulfonate) (PSS) and poly(diallyldimethylammonium) (PDADMA) were here studied with *ab initio* molecular dynamics (AIMD) and classical molecular dynamics (MD) simulations based on the OPLS-aa force-field which is an empirical fixed point-charge force-field. Ion-specific binding to the PE charge groups was also characterized. Both computational methods predict similar response for the

solvation of the PEs but differ notably in description of ion solvation. Notably, AIMD captures the experimentally observed differences in Cl⁻ and Br⁻ anion solvation and binding with the PEs, while the classical MD simulations fail to differentiate the ion species response. Furthermore, the findings show that combining AIMD with the computationally less costly classical MD simulations allows benefiting from both the increased accuracy and statistics reach.

Introduction

Polyelectrolyte complexes (PECs) and multilayers (PEMs) formed from oppositely charged polyelectrolytes (PEs) are closely related in terms of molecular level structure^[1,2] and broadly used in biotechnology, medicine, and chemical engineering as versatile, broadly tunable advanced materials.^[3] Applications include, e.g. drug delivery,^[4,5] tissue engineering,^[6] smart coatings,^[7] electrochemical systems,^[8] water purification,^[9] and drying agents.^[10] The versatility of hydrated PE materials is due to their high sensitivity to the environment. The ionizable functional groups make PEs responsive to various solution conditions, such as salt concentration, pH, temperature, and solvation level.^[11–14] This not only allows a wide spectra of PE material applications but also enables fine-tuning properties and structure of both PECs and PEMs by varying assembly conditions and post-assembly modification.

The solution conditions influence PE assemblies due to changes in polymer mobility and packing in the assembly. Because of this, e.g. the effects of water and salt are coupled.^[15,16] Water plasticizes PE assemblies by enabling enhanced polymer mobility via increasing the free volume and by weakening electrostatic attraction between oppositely charged polyelectrolytes.^[15,17] In this, especially the amount of water hydrating the intrinsic PE–PE ion pairs is important,^[15,18] for further characterization techniques, see e.g. Refs. [17, 19]. The role of salt is more complex, on one hand breaking intrinsic PE–PE ion pairs and weakening the PE–PE interactions and on other hand, binding water.^[15] The salt concentration, i.e. ionic strength has been shown to impact the mechanical properties,^[20] growth profiles,^[21,22] film structure,^[23] water content and swelling,^[24] and glass transition temperature^[15,25] of PEMs. Furthermore, the influence of the salt type has been observed in the PEM structure and properties, such as thickness,^[26–28] swelling,^[29] surface roughness,^[27,30] and stiffness^[31] of the films.

Additional complexity to understanding the response of PE assemblies to the salt rises from the response, quite expectedly, being ion species specific. Ion properties, including the ion size, solvation, and polarizability have an effect on PEM characteristics.^[28,29,32,33] A common rationalization means to the effects of ions on PEs is the Hofmeister series, see e.g. Refs. [34,35]. In PE solutions, complexity to the effects of salt rises from the interplay of solvent molecules, solutes, and ions.^[36] Coupling with the solvation response, ion solvation has been proposed to have a crucial role in ion specificity: For example, Collins *et al.*^[37,38] have shown that strong ion pairing occurs only when ions exhibit similar water affinities. The key role of the solvent affinity to charged species has also been observed in PE systems.^[39,40] For instance, larger, highly polarized ions with weaker solvation shells, such as Br⁻ ion, have been shown to interact more strongly with charged PEs compared to Cl⁻ ion.^[28] Furthermore, differences in the interaction mechanisms between chaotropic and kosmotropic anions with the PE brushes have been observed by Kou *et al.*^[41]

[a] T. Kastinen, D. Tolmachev, K. Laasonen, M. Sammalkorpi
Department of Chemistry and Materials Science, Aalto University, P.O. Box 16100, 00076 Aalto, Finland
E-mail: maria.sammalkorpi@aalto.fi

[b] T. Kastinen, D. Tolmachev, M. Sammalkorpi
Academy of Finland Center of Excellence in Life-Inspired Hybrid Materials (LIBER), Aalto University, P.O. Box 16100, 00076 Aalto, Finland

[c] T. Kastinen
Faculty of Engineering and Natural Sciences, Tampere University, P.O. Box 541, 33014 Tampere University, Finland

[d] P. Batys
Jerzy Haber Institute of Catalysis and Surface Chemistry, Polish Academy of Sciences, Niezapominajek 8, PL-30239 Krakow, Poland

[e] M. Sammalkorpi
Department of Bioproducts and Biosystems, Aalto University, P.O. Box 16100, 00076 Aalto, Finland

Supporting information for this article is available on the WWW under <https://doi.org/10.1002/cphc.202400244>

© 2024 The Authors. ChemPhysChem published by Wiley-VCH GmbH. This is an open access article under the terms of the Creative Commons Attribution License, which permits use, distribution and reproduction in any medium, provided the original work is properly cited.

The balance of hydrophobic/hydrophilic and electrostatic interactions between polymer chain and specific ions on the molecular level dictate the precise structure and properties of the PE material.^[29,42]

Altogether, the existing literature shows that the intrinsic PE–PE ion pairs, extrinsic charge compensation of the PE charge groups by small ions in the solution, and the respective solvations of the charged species and their complexes set the microstructural controls for PE materials properties. However, probing these remains challenging. Molecular simulations offer an efficient, direct approach to such investigation. Indeed, atomistic molecular dynamics (MD) simulations based on empirical force-fields have been employed successfully for investigating the ion-specific effects in the different PEC and PEM systems by us^[19,43–45] and others.^[46,47] The prior works demonstrate that the outcomes of MD simulations can be used to advance mean-field level, such as the classical Poisson–Boltzmann theory, predictions to chemical specificity^[45,46] but also are able to detect the cation specificity^[19] and significant differences in local solvation depending on the chemical species.^[48]

However, these simulations rely on models that describe molecular charge distributions by setting fixed point charges on the atoms to capture an effective charge distribution. Although a justified choice to capture the mean response, and popularized also by the computational efficiency, the fixed partial charges limit by the construction of the modelling accuracy as the approach omits all charge redistribution due to variation in a local environment, i.e. the electronic polarization effects. Additionally, it is worth noting that the fixed partial charges correspond to the parametrization environment, typically a water solution, which increases the inaccuracies in, e.g. apolar environments, see e.g. Refs. [49–51].

For ion interactions in water solutions, recent studies raise attention to force-fields based on fixed point charge values for the ion charge in atomistic detail MD simulations leading to an overestimation of the binding of the ions to the charged species.^[52–54] For PEs, this means that even at very low concentrations of salt, unrealistic ion condensation can occur affecting the solvation size^[52] and local conformations and dynamics of the PEs.^[54] Polarization effects correcting for this can be included by either modifying the existing fixed point charge force-field parameters or by introducing an additional interaction contribution to the force-field, however at the risk of unexpected, artificial outcomes in other assembly features in the system, e.g. in the conformations of PEs.^[53,54] Polarizable force-fields are an option but impose a significant additional computational cost, reducing the feasible system sizes, and additionally suffer from the lack of transferability, requiring tedious parameterization compared to the widely used fixed point charge based traditional force-fields.^[53]

The challenges in force-field based atomistic detail descriptions raise a question, whether quantum mechanics based *ab initio* simulations approaches can at practical level provide additional insight into complex systems such as PE–ion interactions. Static *ab initio* approaches are limited in developing understanding of the hydrated PE–ion pair but *ab initio* MD

(AIMD), where the classical equations of motion are solved by calculating the forces ‘on the fly’ from a first principles electronic structure method hold promise as innately very accurate but computationally costly approach. AIMD simulations have been employed for studying the structure and dynamics of water,^[55–59] the solvation of metal ions in pure water and electrolyte solutions,^[60–69] ionic liquids^[70] and deep eutectic solvents,^[71] interfacial structures,^[72–74] and the interactions between small compounds and ions.^[75,76] This means that the few hundreds of picoseconds and hundreds, perhaps a few thousand atoms, accessible currently by AIMD approaches, see Refs. [69,73,77] for examples of extensive AIMD simulations, have made AIMD a popular tool for studying low molecular weight compounds. AIMD studies of PE systems remain limited to the investigation of photon conduction in PE systems,^[78–80] where both accurate description of the vibrations is needed and relatively short simulation times are sufficient to capture the relevant dependencies. Additionally, recently, we refined empirical force-field based MD simulations results for the solvation and ion distribution around PE molecules by AIMD simulations.^[19] The work demonstrated that AIMD can be used to increase accuracy in interpretation of the experimental results on PE materials in comparison to mere force-field based MD simulations.^[19]

Here, we show that AIMD simulations reach the scale that they can be used to extract useful, high accuracy molecular level information of the microscopic structure and dependencies in PE systems, ion binding to the PE charge groups, and the molecular level solvation dependencies in this. AIMD and classical force-field based MD simulations in capturing the ion-specific effects on both ion binding and on the solvation of two common model PEs, poly(styrene sulfonate) (PSS) and poly(diallyldimethylammonium) (PDADMA) are compared. This particular system is chosen as the AIMD test bed system because our recent work on the same PEs shows that empirical force-field based MD simulations can fail in distinguishing at molecular level the experimentally observed differences in the effects of even simple ions such as Cl[−] and Br[−] ions.^[19] The current work demonstrates that indeed, AIMD can be used to extract high precision information at useful level from this complex system. Additionally, combining classical empirical force-field based MD simulations and AIMD allows overcoming the main drawback of lack of sampling in AIMD, yet achieving enhanced accuracy in solvation shell and ion binding characterization.

Computational Details and Studied Systems

Studied systems. The two common model PEs, PSS and PDADMA were chosen for the study focus because their complexes and assemblies have been extensively studied by us^[15,19,29,48,81–84] and others^[30,85–87] making them a well-characterized, ideal model system for assessing the usability of AIMD as method for such systems and probing the impact of the salt type with a rigorous quantum mechanics based simulations approach. We focus on the monovalent counter ions of the PEs,

Na^+ , K^+ , Cl^- , and Br^- , which are selected based on the salt types (KBr, NaBr, NaCl, and KCl) employed in our previous studies where we studied their effect on PEM swelling^[29] experimentally and on water contents^[19] by both experimental and computational means. The findings demonstrated that the addition of salt leads to the swelling of PSS/PDADMA films, primarily via the interactions between anions and PDADMA. Notably, Br^- ions exerted a more pronounced effect than Cl^- ions on the structure of the PEC due to their chaotropic nature.^[29] The specificity of the interaction between PSS and cations, in turn, governs the solvation of the PEC.^[19] Na^+ ions, which exhibit stronger interactions with the polyelectrolyte, result in lower solvation of the PEC compared to K^+ ions. However, classical force-field based MD simulations failed in distinguishing these AIMD revealed differences in the effects of Cl^- and Br^- ions, despite a clear difference in experimentally measured response.^[19]

Classical MD simulations based on empirical force-field.

The Gromacs package, version 5.1.2,^[88] was used for the all-atom MD simulations. Single PSS and PDADMA chains with 20 repeat units neutralized by Na^+ , K^+ , Cl^- , and Br^- as counterions were examined. To describe the PEs, the OPLS-aa force-field^[89] was used, with the extension for the ammonium group.^[91] The explicit TIP4P water model^[91] was employed for water. The parameters for all the cations are from Ref. [92] and for chloride and bromide ions from Ref. [93] and Ref. [94], respectively. The PSS and PDADMA models have previously been validated against the radius of gyration.^[82] The single polymer chain was placed as a random coil in a cubic simulation box with the box side length 8.7 nm. This significantly exceeds the PE chain radius of gyration for both PEs. Periodic boundary conditions were applied in 3D. The system was solvated by explicit water molecules and neutralized by adding 20 Na^+ , K^+ , Cl^- , or Br^- ions by the Gromacs tools to neutralize the single polymer. After initial energy minimization, the simulations were performed in the NPT ensemble. The V-rescale thermostat^[95] with coupling constant 0.1 ps was applied with a reference temperature $T = 300$ K. The isotropic Parrinello-Rahman barostat^[96] with the coupling constant 1 ps and reference pressure 1 bar was used for pressure control. The long-range electrostatic interactions were calculated using the PME method.^[97] Van der Waals interactions were described using the Lennard-Jones potential with a 1.0 nm cut-off. All the bonds in the PEs and water molecules were controlled by the LINCS^[98] and SETTLE^[99] algorithms, respectively. A 2 fs time step within the leap-frog integration scheme was applied and the trajectories were written every 1 ps. The first 20 ns of the simulation were considered as an equilibration of the system and disregarded from the analysis. The production run corresponded to the subsequent 50 ns.

AIMD simulations. Four different systems consisting of one PE trimer model (PSS or PDADMA) and one counter ion (Na^+ , K^+ , Cl^- , or Br^-) with water molecules were simulated in cubic $(2.5 \text{ nm})^3$ simulation boxes (Figure 1). The initial configurations for the AIMD simulations were obtained by extracting a representative PE trimer segment from the final 50 ns configuration of the classical MD simulation of the 20-mer PE, one

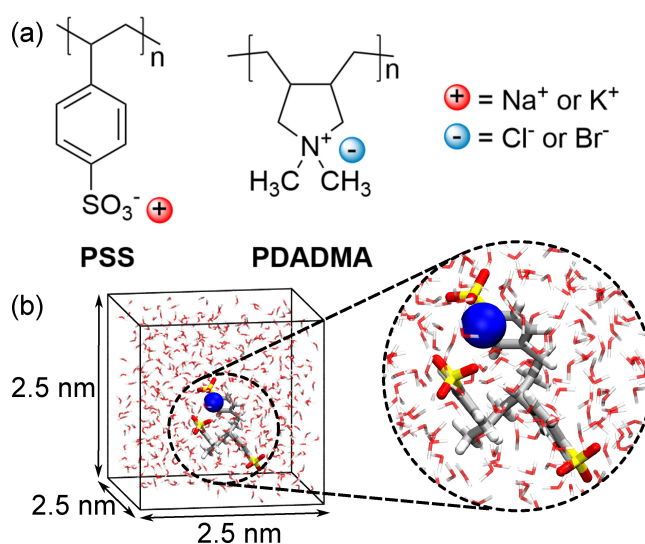


Figure 1. (a) Chemical structures of the studied PEs with counter ions and (b) a representation of an initial AIMD simulation configuration for the PSS trimer and a single Na^+ ion in a $(2.5 \text{ nm})^3$ simulation box.

counter ion closest to the PE trimer charge groups (between the charge groups), and a surrounding water shell ca. 1 nm in thickness around the extracted species. The missing hydrogens were added to the chain ends of the extracted PE trimers. Locally, the PE side chains adopt spatial arrangements dominated by the electrostatic repulsion between the neighboring PE charged groups. Although overall chain conformations in 20-mers and trimers differ, the water shell around the charge groups in trimers is similar to longer chains. The number of water molecules in the PE–ion systems was adjusted to reach the experimental water density in the ambient conditions in the $(2.5 \text{ nm})^3$ simulation boxes (ca. 1 g cm^{-3}). The total number of water molecules was 481 for PSS–ion systems and 500 for PDADMA–ion systems. Additionally, ‘ion-only’ systems consisting of one single counter ion (Na^+ , K^+ , Cl^- , or Br^-) and 255 explicit water molecules in cubic $(1.9734 \text{ nm})^3$ simulation boxes with the density of ca. 1 g cm^{-3} were studied for comparison. These ion-only systems correspond to the ‘free’ counter ions in the bulk water of the PE–ion systems in the classical MD simulations.

The (Born–Oppenheimer) AIMD simulations were carried out by using the Quickstep module^[100] of the CP2K software.^[101] Electronic structure calculations were carried out with Kohn–Sham density functional theory (DFT) using a hybrid Gaussian and plane waves method.^[101] Due to a good balance between accuracy and computational cost, the Kohn–Sham formulation of the DFT has been a popular choice for the theory approach underlying the AIMD dynamics. The PBE exchange–correlation functional^[102] was employed in conjunction with dispersion corrections introduced by the DFT–D3(BJ) method.^[103,104] Previous studies have highlighted the importance of accounting for the van der Waals interactions in accurate description of ion–water and water–water interactions.^[59] The molecularly optimized double- ζ -DZVP-MOLOPT-SR-GTH basis set^[105] with the Goedecker–Teter–Hutter pseudopotentials were

used for all atom types.^[106–108] A plane wave cut-off of 600 Ry was employed with a reference grid cut-off of 50 Ry. The Kohn-Sham equations were solved by using the orbital transformation method^[109] with a DIIS minimizer and a FULL SINGLE INVERSE preconditioner. An SCF convergence criterion of 10^{-6} a.u. was used. The net charge of the system (PSS-ion: $-2e$, PDADMA-ion: $+2e$, single cation: $+e$, and single anion: $-e$), was neutralized by a homogeneous background charge distribution applied automatically in CP2K. This approach approximates the remaining two counterions as delocalized effective charge, which is a more accurate approximation than bringing into the AIMD simulation system three explicit, spatially localized ions. Periodic boundary conditions were applied in all directions.

The systems were first geometry optimized by using the LBFGS algorithm.^[110] After this, the AIMD simulations were carried out in the NVT ensemble at a reference temperature 348.15 K maintained by the velocity rescaling CSRV thermostat.^[95] The AIMD simulations used a higher temperature to avoid the overstructuring of water previously reported characteristic to the PBE functional.^[73,111] A time step of 1 fs was used with the Velocity-Verlet integrator.^[112] The systems were first equilibrated for 10 ps during which strong thermostating was implemented by using a time constant of 50 fs. After this, the thermostat time constant was increased to 100 fs and the equilibration was continued for 10–15 ps. This was followed by 60 ps production runs, analyzed for the results. The trajectories were written every 5 ps.

Analysis. All presented simulation visualizations are by the VMD software package.^[113] For the classical MD simulations, the radial distribution functions (RDFs), $g(r)$, and the corresponding cumulative number count RDFs were calculated using the built-in Gromacs tools. The AIMD RDFs, corresponding cumulative number count RDFs, and both the classical MD and AIMD coordination number distributions were determined with the VMD software,^[113] while the angular distribution analyses were carried out with MDAnalysis 2.3.0.^[114,115] The single coordination number values of the first solvation shells around the ions and PE charge groups presented in ESI† were obtained by integrating the RDFs up to the first minimum. For coordination number distributions, an in-house VMD script was used for calculating the number of water molecules within the first

solvation shell. The first RDF minima were used as the cut-off values for calculating the coordination number and angular distributions, see Tables S1–S5 in ESI†.

Results and Discussion

Solvation of the polyelectrolytes. First, we investigated the aqueous solvation environment of the two PEs with Na^+ , K^+ , Cl^- , and Br^- ions both by the AIMD and classical MD simulations. Figure 2 presents the visualizations of the first water solvation shells in the PE-ion systems of the AIMD simulations. Quantitative characterization of the molecular level solvation structure is by RDFs between the PE charge groups and water in Figure 3 where data for both AIMD and the classical MD simulations is shown. Contributions from water oxygen O and hydrogens H are separated to allow differentiating water ordering by the data. The corresponding numerical data for both AIMD and MD simulations are given in Tables S1 and S2 in the ESI†, respectively. In general, PSS and PDADMA have notably different water distributions around their charge groups. Both AIMD and the classical MD simulations result in the PE–O RDFs of PSS having a prominent main peak associated with the first solvation shell. The two smaller peaks indicate the presence of the second and third solvation shells. Opposed to this, for PDADMA, only two peaks, the first and second solvation shell, are observed in the PE–O RDFs. Additionally, the PDADMA peaks are at larger distances, reflecting the chemical structure of the charged functional group (more bulky for PDADMA). In line with this, the RDF peak position and height indicate that the first solvation shell of PSS is smaller and the water molecules are more tightly bound to the PSS charge groups compared to PDADMA. Also, this different affinity of the PEs to water can be connected to the chemical nature of their charge groups: hydrophilic sulfonate groups in PSS draw water molecules closer and form hydrogen bonds with them,^[15] while hydrophobic methyl groups in PDADMA will push water further from them.

The solvation shells of the PE charge groups simulated by AIMD and the classical MD are similar. In the PE–water RDFs, the AIMD simulations show slightly more difference between

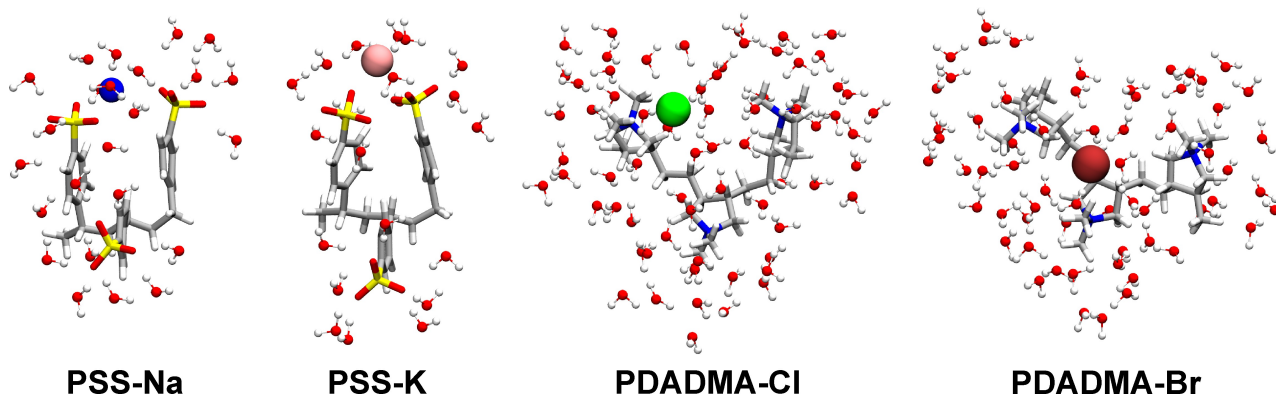


Figure 2. Molecular visualizations of the AIMD PE-ion systems. Only the water molecules in the first solvation shells of the PE charge groups and the counterions are shown.

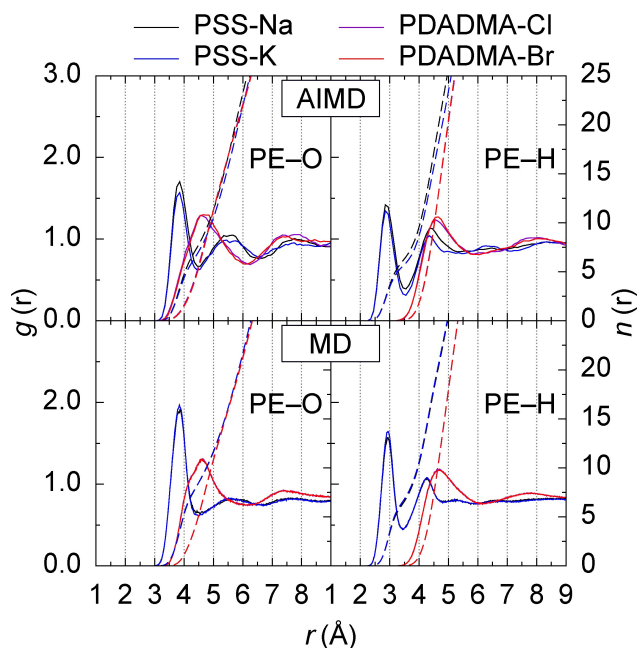


Figure 3. Radial distribution function $g(r)$ and the corresponding cumulative number counts $n(r)$ calculated between the center atoms of the PE charge groups (S atoms in PSS and N atoms in PDADMA) and water oxygens (PE–O) and hydrogens (PE–H) in the PE–ion systems. Data for both the AIMD and the classical MD simulations is presented.

the different types of ions compared to the classical MD. Calculation of the explicit number of water molecules in the first solvation shell of the PE charge group shows that more water molecules are present in the first solvation shell of the PE charge group for the Na^+ than the K^+ cation and for the Cl^- than the Br^- anion (Table S1, ESI†). This can be attributed to the ions binding to different positions and distances from the PE chain. Notably, AIMD predicts that Na^+ and Cl^- ions are located farther away from the PE charge groups than the K^+ and Br^- ions during the first 50 ps of the simulation. This leads to a smaller impact on the solvation shell of PEs (see Figure S1–S3 in ESI†). Except for the ion species dependency on the solvation, AIMD and the classical MD show the same solvation response for the PE charge groups.

The water structure in the first solvation shells of the PE charge groups was further assessed by the orientations of water molecules around the charge groups. The distributions of the angle θ (angle $\angle \text{M}\cdots\text{O}-\text{H}$) are presented in Figure S4 (ESI†, see the same figure also for schematic of the angle). The two different computational methods predict similar trends for the orientation of water molecules around the PSS charge groups: One major orientation peak is at ca. $16\text{--}18^\circ$ with both AIMD and MD. This means that a hydrogen in water molecules is pointing toward the PSS charge group due to the hydrogen bonding between PSS and water. In the case of PDADMA, however, the peak position differs between the AIMD and MD simulations: The major orientation peak is at ca. $61\text{--}71^\circ$ with AIMD and at ca. 76° with MD. This results from the water oxygens being attracted to the positive charge of the PDADMA.

The ion type does not have a significant effect on the orientation of water molecules around the PE charge groups.

Solvation of the counter ions. Further comparison of the ion solvation responses shows that even though AIMD and classical MD simulations were very similar in the representation of PE solvation, the ion solvation descriptions differ significantly. A comparison of the predicted RDFs between the ions and water for the ions providing extrinsic charge compensation with the PE charge groups is presented in Figure 4. The corresponding data for the ions in bulk solution are presented in Figure S5 (ESI†). Numerical data values extracted from the AIMD RDFs are collected in Tables S3 and S4, while those from classical MD simulations are in Table S5 (ESI†). The data shows that in the AIMD simulations, the size of the first solvation shell of both the ions providing extrinsic charge compensation and the ions in bulk solution increases in the order of $\text{Na}^+ < \text{K}^+ < \text{Cl}^- < \text{Br}^-$ (Figure 4 and S5(a), ESI†). This correlates directly with the ionic radii, increasing with ion size.^[116,117]

The calculated ion–O distances for the solvation shell of the bulk ions in the AIMD simulations are also in good agreement with experimental values for monovalent ions determined by EXAFS, neutron diffraction, and large angle X-ray scattering (LAXS) (Na^+ : 2.37, 2.38 Å,^[118] K^+ : 2.81 Å,^[119] Cl^- : 3.05–3.16 Å,^[120–122] Br^- : 3.30 Å^[123]) and also those obtained in previous AIMD simulations (Na^+ : 2.41 Å,^[65] K^+ : 2.80 Å,^[65] 2.82 Å,^[59] Cl^- : 3.11 Å,^[60] 3.12 Å,^[60] Br^- : 3.33 Å^[124]). On the other hand, the ion–O distances describing the water shell in the classical MD simulations come out slightly larger for Na^+ and Cl^- and smaller for K^+ and Br^- compared to AIMD. In our previous work,

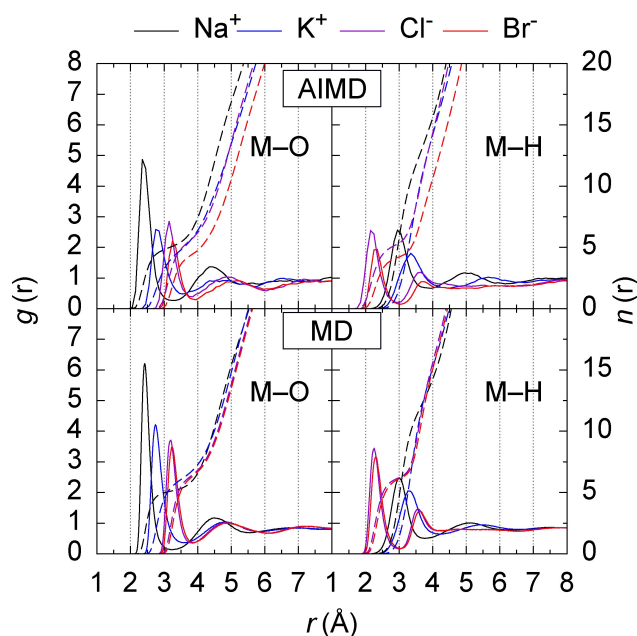


Figure 4. Radial distribution function $g(r)$ and the corresponding cumulative number counts $n(r)$ calculated between the counter ions and water oxygens (M–O) and hydrogens (M–H) in the PE–ion systems. Data for both the AIMD and the classical MD simulations is presented. For MD simulations, only the counter ions within the 7 or 6 Å cut-off distance from the PSS and PDADMA charge group center atoms, respectively, have been considered. Corresponding data for the ions in bulk water is presented in ESI†, in Figure S5.

corresponding classical MD simulations could not capture a difference evident in experimental data:^[19] we note that the here observed slight overestimation of the contact distance between water and Cl^- ion and underestimation of Br^- ion water distance in the classical MD model eliminates the difference in solvation shell structure for these anions affecting also the coordination numbers (Tables S3 and S4, ES†). The presence of a PE does not have a significant effect on the ion–water distances. However, the peak heights corresponding to the ions providing extrinsic charge compensation to the PE and the ions in bulk solution differ, reflecting coordination number differences at a given distance. In the classical MD simulations, the peak intensities of the RDFs for the ions providing extrinsic charge compensation and water are smaller than those calculated for the ions in bulk solution vs water. Contrary to this, AIMD does not show significant difference.

Overall, the coordination numbers predicted for the water molecules in the first solvation shell of bulk ions by AIMD simulations (Table S4) correlate well with those predicted

experimentally (Na^+ : 5.5,^[118] K^+ : 7.0,^[119] Cl^- : 6.0–6.9,^[120–122] Br^- : 6.9^[125]). However, the atomistic detail classical MD simulations overestimate the bulk ion coordination numbers slightly, except for K^+ (Table S5). In line with the observations of ion–water molecule distance response, where the distance of Br^- was underestimated and Cl^- overestimated, the classical MD simulations with the employed ion models do not show a significant difference in the coordination number for Br^- and Cl^- ions (see the cumulative RDFs in Figure 4 and S5). Both computational methods show that the presence of the PE decreases the ion solvation shell coordination numbers for the ions providing extrinsic charge compensation in comparison to the ions in the bulk solution. This is because of the close contact between the ion and the PE charge groups.

The size of the first solvation shell in water molecules fluctuates in time, resulting in a distribution of the solvation shell coordination numbers of the water molecules calculated for the counter ions. The data for both AIMD and classical MD simulations are presented in Figure 5. AIMD predicts a narrow

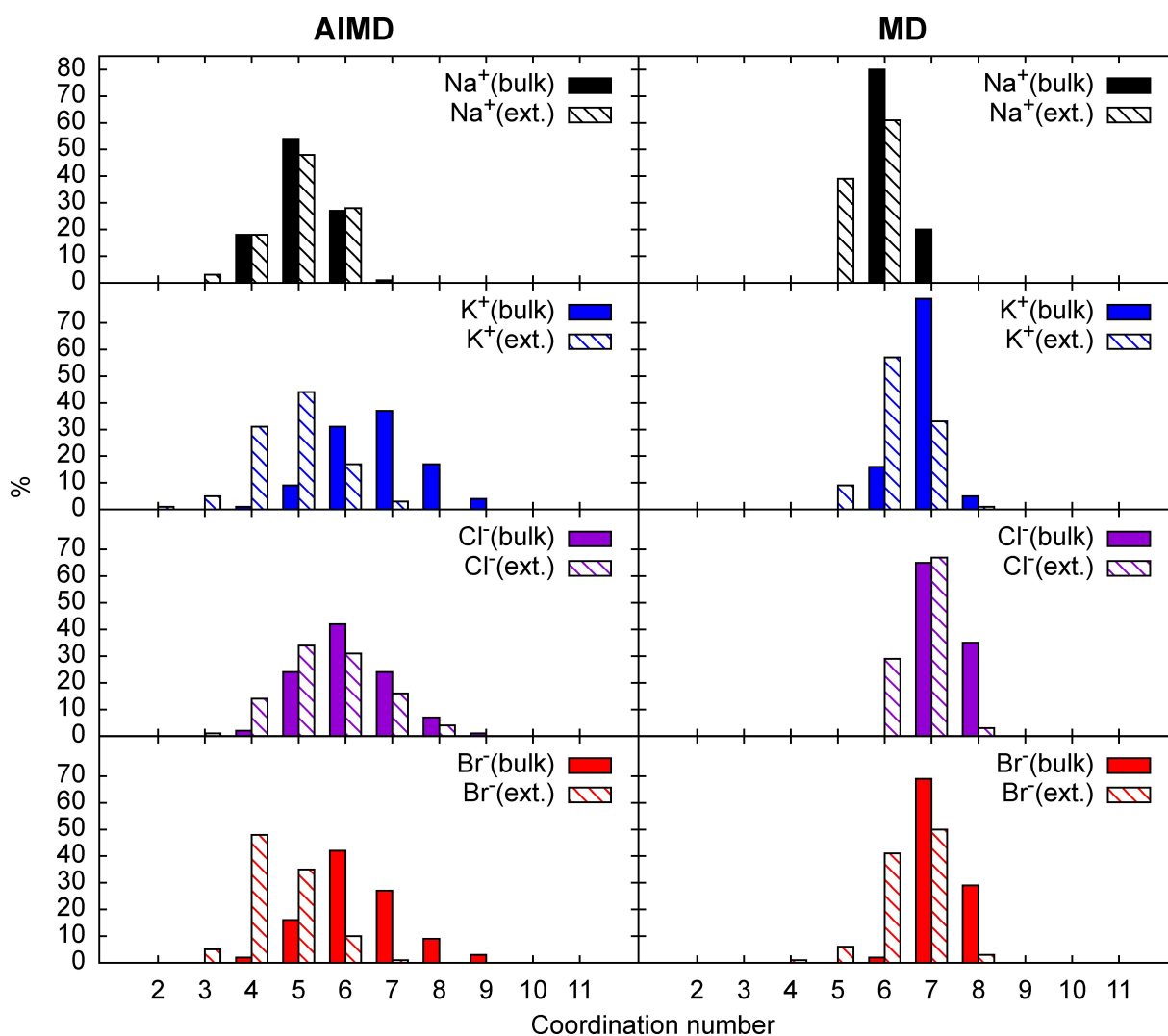


Figure 5. Percentage distributions of water molecule coordination numbers in the first solvation shells of the counter ions. Data for the ions providing extrinsic charge compensation to the PE (ext.) and the ions in bulk water (bulk) based on both the AIMD and MD simulations is presented. The AIMD data for the bulk ions is from the ion-only systems.

and sharp distribution for Na^+ in line with the ion–O RDFs (Figure 4 and S5). This indicates a smaller and more compact first solvation shell in comparison to the other ions. The larger K^+ , Cl^- , and Br^- ions have more significant fluctuations in terms of number of water molecules around them. This leads to broader water molecule coordination number distributions for the ions, i.e. more loosely packed solvation shells. This can affect the interaction between the ion and PE (Figure 7).^[28] The distribution profiles of the ions in bulk solution predicted by AIMD simulations are consistent with those predicted with the NS and WAXS scattering measurements.^[126] The effect of the PE presence can be clearly seen in the coordination number distributions for all ions, with the distributions shifted toward smaller coordination numbers in the data corresponding to the ions providing extrinsic charge compensation in comparison to the ions in bulk water. The ions with low solvation energies (K^+ and Br^-) lose more water molecules from their solvation shells when the ion is interacting with a PE. The finding can explain the larger swelling of PSS/PDADMA PEMs when these ions are present in the solution.^[19,29] In contrast to AIMD simulations, classical MD simulations with the employed ion models predict narrow coordination number distributions for all ions. As already stated for the priorly measured quantities, also here the difference between the examined anions is less notable in the classical MD simulations for the ions providing extrinsic charge compensation than with AIMD simulations. This is related to an inaccurate Br^- model in the OPLS force-field.^[127]

Angular distributions of water molecules for both the ions providing extrinsic charge compensation and the ions in bulk solution calculated with the AIMD and the classical MD simulations show that all studied ions have a strong orienting

influence on water in their first solvation shell (see Figure 6). The strength of orientation differs slightly between the AIMD and MD simulations for the anions, which have one major peak at ca. 13° . This indicates that the water hydrogens in the first solvation shell, quite expectedly, point towards anions. The cations lead to a very similar water ordering effect using both models with the major peak at ca. 105° . This corresponds, again expectedly, to the water oxygens pointing towards the cations. Correspondingly, the water hydrogens point outward. Also the ion–H distances (Figure 4(b) and S5(b)) reflect this, with the anions having shorter separation from the hydrogens than the cations. The orientation distributions of water molecules are very similar for the cations providing extrinsic charge compensation to the PE and those in the bulk, i.e. the presence of a PE does not have much impact on the water orientation around the ions binding to the charge groups. Interestingly, the orientation of water molecules is more similar for Cl^- and Br^- than for Na^+ and K^+ . The classical MD simulations predict similar trends as the AIMD modelling, although some difference in the peak positions between the two computational methods exists.

Polyelectrolyte–ion interactions. The RDFs between the PE charge group and the counter ion provide insight into the PE–ion interactions (see Figure 7). The AIMD simulations indicate that the distances between the PE charge group and the counter ion increase in the order of $\text{Na}^+ < \text{K}^+ < \text{Cl}^- < \text{Br}^-$. This indicates that the binding of cations to the PSS charge group is stronger than the PDADMA–anion binding. The classical MD simulations predict the same ordering for the cations, but for the anions, the PE–ion distances are predicted to be nearly identical in the classical MD simulations modelling.

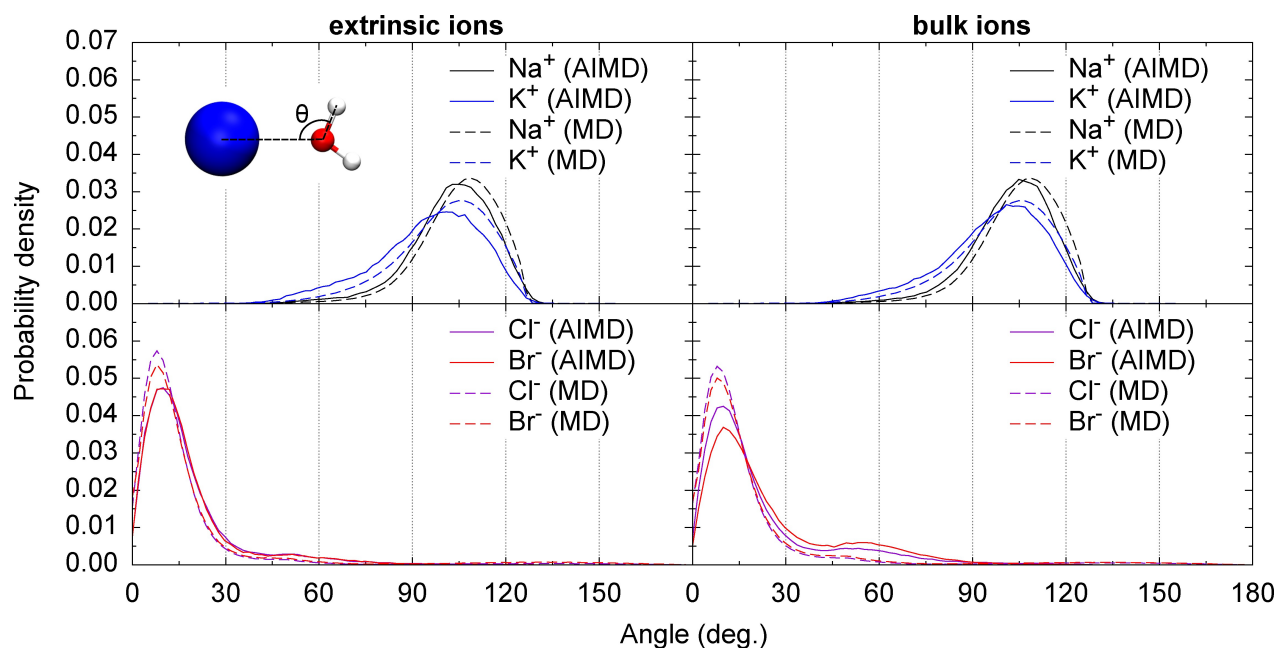


Figure 6. Angular orientation distributions of water molecules in the first solvation shells of the ions based on the AIMD and classical MD simulations. Data for the ions providing extrinsic charge compensation to the PE, extrinsic ions (PE–ion systems in AIMD), and freely solvated ions, bulk ions (ion-only systems in AIMD), are presented. The $\angle \text{M}\cdots\text{O}-\text{H}$ angle θ between the ion M and water is considered, see inset. Only the angles formed via the water hydrogens closest to an ion are considered.

The time evolutions of the PE–ion distances with AIMD (Figure S1, ESI†) show that for the PSS–Na system, the ion is first at a larger separation distance from the charge groups but then moves closer to one of the charge groups. The ion has an average distance of ca. 3.6 Å during the last 10 ps of the AIMD simulation. Opposed to this, K⁺ is mostly shared by two PSS charge groups. The larger size of the charge groups and anions in the PDADMA systems leads to the ions preferring binding configuration in which they are shared by all three charge groups in the AIMD modelling.

It is important to note that the lifetime of the ion/PE contact, especially for the Na⁺ ions, exceeds the time scale of the AIMD modelling here. This means the sampling is not sufficient for accurately reproducing the relative probabilities of different binding states in the system. On the other hand, the AIMD modelling reproduces contact distances between ions and the PE more accurately than the classical MD simulations model (at a given binding configuration). In line with the ion solvation results, the contact distance of the ion to the charge group predicted by AIMD simulations is smaller than the classical MD simulations predicted distances. Also, in contrast to MD simulations, the AIMD modelling is able to differentiate the two anions in their binding. This is because the ion solvation shell is more accurately represented (see Figure 4). The Br[−] ions interact energetically more favorably with the PE charge group than the Cl[−] ions. This is primarily due to the lower solvation energy of Br[−]. Another notable difference between the classical MD and AIMD simulations is the difference in the height of the first binding peak in the RDF calculated for the cations and PE charge groups (Figure 7). This is especially true for Na⁺. The classical MD simulations predict a much stronger binding than the AIMD simulations. Indeed, this is well known: most classical

fixed point charge force-fields describe Na⁺ ions such that they exhibit overbinding.^[52] Modifying the ion model can rectify this particular inaccuracy in the model, but it can also introduce other issues in model accuracy.^[52,54]

Conclusions

We demonstrated here that AIMD simulations can be used to examine complex, hydrated charge groups and ion-binding systems such as PEs and their counterions. To this purpose, the ion-specific effects on the solvation and ion binding of two common PEs, PSS and PDADMA, with Na⁺, K⁺, Cl[−], and Br[−] as the counterions were studied. Comparing AIMD and atomistic detail MD based on a fixed-point charge empirical force-field, showed that overall, the two approaches differed significantly in ion solvation descriptions but predicted very similar solvation responses for the PE charge groups; the general water description accuracy in the AIMD methodology is assessed in Ref. [129]. In ion interactions with the PE charge groups, the AIMD simulations showed a larger difference between the ions than the MD simulations. For the ion solvation response that had significant differences between the modelling approaches, the AIMD simulations results of the ion-water molecule distances and coordination numbers are in line with experiments, while the classical MD simulations result in values that are slightly overestimated/underestimated. The study also showed that the water coordination number distributions calculated for the solvation shell size of the ions are also narrower for the classical MD simulations than those calculated based on the AIMD approach. Especially, the classical MD simulations show less notable difference between the solvation description of the anions.

The two computational methods have also significant differences in capturing the ion binding to the PE charge group. While the sampling is not sufficient for describing the relative probabilities of different binding states in the AIMD simulations, AIMD still provides more accurate PE–ion contact distances at a given binding configuration compared to the classical MD simulations. Following the findings on the solvation of ions, the AIMD approach is able to differentiate the monovalent anions, while the classical MD simulations predict nearly identical binding states for them. In addition, the classical MD shows stronger cation binding than AIMD, especially for Na⁺, due to well known overbinding problem in the most classical fixed point charge force-fields.

The significance of the performed comparison and the findings is that modern AIMD approaches have the reach to accurately model solvated PE–ion systems. Furthermore, the data shows that AIMD provides significant accuracy gain for especially the hard, small ions such as Na⁺; indeed the classical MD point charge approximation is able to model the somewhat larger ions in better agreement with the AIMD data. Demonstrated here by the AIMD's ability to capture anion binding difference between Cl[−] and Br[−] such that experimentally measured trends in PE materials swelling and binding response can be explained, the work shows that AIMD brings in

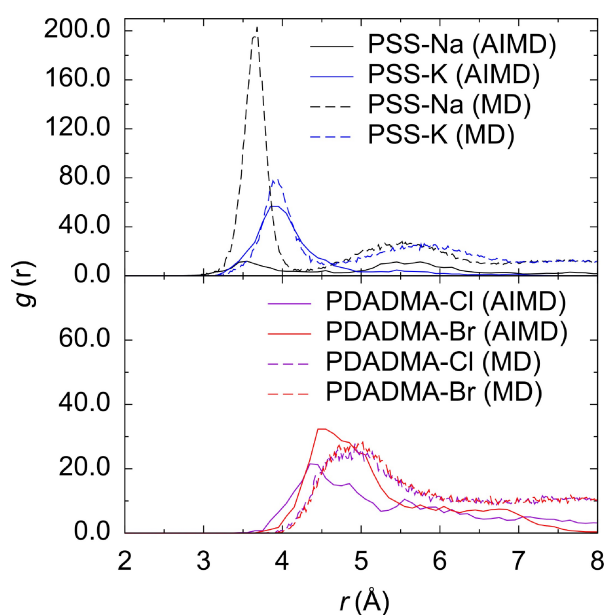


Figure 7. Radial distribution function $g(r)$ calculated between the PE charge group central atoms (S atoms in PSS and N atoms in PDADMA) and the counterion. Data for both the AIMD and the classical MD simulations are presented.

quantitative comparison to experimental observations via the increased accuracy. This means that when in need of high accuracy, AIMD is an actual option. AIMD can bring significant gains in the prediction ability of computational modelling in comparison to classical MD. Here, the major bottleneck in MD prediction ability is its inability to reproduce the electrostatic interactions with sufficient accuracy. Polarizable potentials in classical MD force-fields improve the accuracy of MD simulations in this sense significantly.^[129] However, despite the recent active pursuit to develop polarizable force-fields for different compounds,^[129–133] polarizable force-fields still suffer from lack of transferability. This means that the implementation of polarizable potential to a new system with a different environment requires additional validation and parameterization. Moreover, recent studies have shown that even with direct accounting for polarizability, classical MD simulations face challenges in achieving AIMD accuracy in the characterization of local structures for electrolyte systems.^[134]

Generalizing, our findings show that AIMD simulations can be used as a tool to study and analyze complex, multi-component systems under aqueous solvation – here demonstrated for the ion-specific solvation and charge-charge interactions in PE–ion systems. Further, reach for the AIMD simulations that remain lacking in sampling can be achieved by combining classical MD sampling and the AIMD local microstructural characterization. In this work, this made a difference particularly in capturing the solvation and ion binding characteristics, especially for the anions, accurately. Overall, the performed work and the findings set AIMD as a feasible tool for extracting information on solvated, charged systems.

Supporting Information

Supporting information contains additional analysis data from the AIMD and MD simulations: The AIMD and MD simulations RDF analysis data of the hydration shell structure of the PE charge groups in the different systems. Time dependency of the distance between different PE charge groups and the counter ions in the AIMD production runs. Time dependency of the number of water molecules in the PE charge groups first hydration shell in AIMD production runs. Coordination number percentage distributions between the S1 charge group of PSS and water oxygens. Angular orientation distributions of water molecules in the first solvation shells of the PE charge groups for PSS–ion and PDADMA–ion systems. Radial distribution function $g(r)$ and cumulative number count $n(r)$ calculated between the counter ions and water oxygens and hydrogens in the AIMD and MD simulations. AIMD and MD simulations based numerical data corresponding to the RDF analysis as tables.

Author Contributions

Tuuva Kastinen: conceptualization, investigation, formal analysis, software, data curation, writing – original draft, visualization. Piotr Batys: investigation, formal analysis, software, data

curation, writing – original draft. Dmitry Tolmachev: formal analysis, software, writing – original draft. Kari Laasonen: conceptualization, instructioning, writing – review & editing. Maria Sammalkorpi: conceptualization, supervision, funding acquisition, resources, project administration, writing – review & editing.

Acknowledgements

This work is supported by the Academy of Finland through its Centres of Excellence Programme (2022–2029, LIBER) under project no. 346111 and 364205 (M.S.) and Academy of Finland project no. 359180 (M.S), Novo Nordisk Foundation under project no. NNF22OC0074060 (M.S.), Finnish Cultural Foundation (T.K.), and National Science Centre, Poland under Grant No. 2018/31/D/ST5/01866 (P.B.). We are grateful for the support by the FinnCERES Materials Bioeconomy Ecosystem. Computational resources by CSC IT Centre for Finland, Poland's high-performance computing infrastructure PLGrid (HPC Centers: ACK Cyfronet AGH), grant no. PLG/2023/016229, and RAMI – RawMatters Finland Infrastructure are also gratefully acknowledged.

Conflict of Interests

The authors declare no conflict of interest.

Data Availability

Data associated with the manuscript, including simulation input files and number data for the figures are available at <https://doi.org/10.23729/ae2bec70-23f5-4466-b6a7-8270a014e60e>

Keywords: *ab initio* molecular dynamics · molecular modelling · polyelectrolyte · poly(diallyldimethylammonium) · poly(styrene sulfonate)

- [1] S. A. Sukhishvili, E. Kharlampieva, V. Izumrudov, *Macromolecules* **2006**, 39, 8873.
- [2] B. P. Das, M. Tsianou, *Adv. Colloid Interface Sci.* **2017**, 244, 71.
- [3] M. Cohen Stuart, W. T. S. Huck, J. Genzer, M. Müller, C. Ober, M. Stamm, G. B. Sukhorukov, I. Szleifer, V. V. Tsukruk, M. Urban, F. Winnik, S. Zauscher, I. Luzinov, S. Minko, *Nat. Mater.* **2010**, 9, 101.
- [4] S. Casey-Power, R. Ryan, G. Behl, P. McLoughlin, M. E. Byrne, L. Fitzhenry, *Pharmaceutica* **2022**, 14, 1479.
- [5] J. Potaś, K. Winnicka, *Int. J. Mol. Sci.* **2022**, 23, 3496.
- [6] M. Suneetha, K. M. Rao, S. S. Han, *Int. J. Biol. Macromol.* **2020**, 144, 160.
- [7] T. Kruk, M. Gołda-Cępa, K. Szczepanowicz, L. Szyk-Warszyńska, M. Brzyczczyn-Włoch, A. Kotarba, P. Warszyński, *Colloids Surf. B* **2019**, 181, 112–118.
- [8] M. Elzbieciak-Wodka, M. Kolasieńska-Sojka, P. Warszyński, *J. Electroanal. Chem.* **2017**, 789, 123.
- [9] J. K. Bediako, J.-H. Kang, Y.-S. Yun, S.-H. Choi, *ACS Appl. Polym. Mater.* **2022**, 4, 2346.
- [10] J. Akintola, Z. A. Digby, J. B. Schlenoff, *ACS Appl. Mater. Interfaces* **2023**, 15, 9962.
- [11] Y. Ghimire, A. Bhattarai, *Int. J. Energy Res.* **2020**, 9, 876.

- [12] N. Wanasingha, P. Dorishetty, N. K. Dutta, N. R. Choudhury, *Gels* **2021**, *7*, 148.
- [13] T. Kruk, K. Chojnacka-Górka, M. Kolasińska-Sojka, S. Zapotoczny, *Adv. Colloid Interface Sci.* **2022**, 102773.
- [14] H. Li, S. M. Lalwani, C. I. Eneh, T. Braide, P. Batys, M. Sammalkorpi, J. L. Lutkenhaus, *Langmuir* **2023**, *39*, 14823.
- [15] Y. Zhang, P. Batys, J. T. O'Neal, F. Li, M. Sammalkorpi, J. L. Lutkenhaus, *ACS Cent. Sci.* **2018**, *4*, 638.
- [16] M. Yang, J. Shi, J. B. Schlenoff, *Macromolecules* **2019**, *52*, 1930.
- [17] J. B. Schlenoff, A. H. Rmaile, C. B. Bucur, *J. Am. Chem. Soc.* **2008**, *130*, 13589.
- [18] P. Batys, Y. Zhang, J. L. Lutkenhaus, M. Sammalkorpi, *Macromolecules* **2018**, *51*, 8268.
- [19] C. I. Eneh, T. Kastinen, S. Oka, P. Batys, M. Sammalkorpi, J. L. Lutkenhaus, *ACS Polym. Au* **2022**, *2*, 287.
- [20] C. H. Porcel, J. B. Schlenoff, *Biomacromolecules* **2009**, *10*, 2968.
- [21] E. Guzmán, H. Ritacco, J. E. F. Rubio, R. G. Rubio, F. Ortega, *Soft Matter* **2009**, *5*, 2130.
- [22] K. Tang, N. A. M. Besseling, *Soft Matter* **2016**, *12*, 1032.
- [23] R. A. McAloney, M. Sinyor, V. Dudnik, M. C. Goh, *Langmuir* **2001**, *17*, 6655.
- [24] S. Doodoo, R. Steitz, A. Laschewsky, R. von Klitzing, *Phys. Chem. Chem. Phys.* **2011**, *13*, 10318.
- [25] J. T. O'Neal, K. G. Wilcox, Y. Zhang, I. M. George, J. L. Lutkenhaus, *J. Chem. Phys.* **2018**, *149*, 163317.
- [26] S. T. Dubas, J. B. Schlenoff, *Macromolecules* **1999**, *32*, 8153.
- [27] M. Salomäki, P. Tervasmäki, S. Areva, J. Kankare, *Langmuir* **2004**, *20*, 3679.
- [28] J. E. Wong, H. Zastrow, W. Jaeger, R. von Klitzing, *Langmuir* **2009**, *25*, 14061.
- [29] J. T. O'Neal, E. Y. Dai, Y. Zhang, K. B. Clark, K. G. Wilcox, I. M. George, N. E. Ramasamy, D. Enriquez, P. Batys, M. Sammalkorpi, J. L. Lutkenhaus, *Langmuir* **2018**, *34*, 999.
- [30] J. Jukić, K. Korade, A.-M. Milisav, I. D. Marion, D. Kovačević, *Coll. Int.* **2021**, *5*, 38.
- [31] M. Salomäki, T. Laiho, J. Kankare, *Macromolecules* **2004**, *37*, 9585.
- [32] W. J. Dressick, K. J. Wahl, N. D. Bassim, R. M. Stroud, D. Y. Petrovykh, *Langmuir* **2012**, *28*, 15831.
- [33] Z. Yu, K. Li, W. Wang, H. Jin, Y. Ge, F. Xiao, H. H. Wu, J. Gong, *Colloid Polym. Sci.* **2022**, *300*, 813–823.
- [34] R. A. Ghostine, R. F. Shamoun, J. B. Schlenoff, *Macromolecules* **2013**, *46*, 4089.
- [35] M. Salomäki, J. Kankare, *Macromolecules* **2008**, *41*, 4423.
- [36] B. Kang, H. Tang, Z. Zhao, S. Song, *ACS Omega* **2020**, *5*, 6229.
- [37] K. D. Collins, *Methods* **2004**, *34*, 300.
- [38] K. D. Collins, *Biophys. Chem.* **2006**, *119*, 271.
- [39] Y. Zhang, P. S. Cremer, *Curr. Opin. Chem. Biol.* **2006**, *10*, 658, model systems / Biopolymers.
- [40] J. Smiatek, *Molecules* **2020**, *25*, 1661.
- [41] R. Kou, J. Zhang, T. Wang, G. Liu, *Langmuir* **2015**, *31*, 10461.
- [42] M. Qiu, S. Long, B. Li, L. Yan, W. Xie, Y. Niu, X. Wang, Q. Guo, A. Xia, *J. Phys. Chem. C* **2013**, *117*, 21870.
- [43] H. S. Antila, M. Sammalkorpi, *J. Phys. Chem. B* **2014**, *118*, 3226.
- [44] H. S. Antila, M. Härkönen, M. Sammalkorpi, *Phys. Chem. Chem. Phys.* **2015**, *17*, 5279.
- [45] P. Batys, S. Luukkonen, M. Sammalkorpi, *Phys. Chem. Chem. Phys.* **2017**, *19*, 24583.
- [46] J. Heyda, J. Dzubiella, *Soft Matter* **2012**, *8*, 9338.
- [47] A. Narayanan Krishnamoorthy, C. Holm, J. Smiatek, *Soft Matter* **2018**, *14*, 6243.
- [48] P. Batys, S. Kivistö, S. M. Lalwani, J. L. Lutkenhaus, M. Sammalkorpi, *Soft Matter* **2019**, *15*, 7823.
- [49] S. Vierros, M. Sammalkorpi, *J. Chem. Phys.* **2015**, *142*, 094902.
- [50] S. Vierros, M. Sammalkorpi, *Phys. Chem. Chem. Phys.* **2015**, *17*, 14951.
- [51] M. Vuorte, S. Kuitunen, M. Sammalkorpi, *Phys. Chem. Chem. Phys.* **2021**, *23*, 21840.
- [52] D. A. Tolmachev, O. S. Boyko, N. V. Lukasheva, H. Martinez-Seara, M. Karttunen, *J. Chem. Theory Comput.* **2020**, *16*, 677.
- [53] E. Duboué-Dijon, M. Javanainen, P. Delcroix, P. Jungwirth, H. Martinez-Seara, *J. Chem. Phys.* **2020**, *153*, 050901.
- [54] N. Lukasheva, D. Tolmachev, H. Martinez-Seara, M. Karttunen, *Polymer* **2022**, *14*, 252.
- [55] L. Ruiz Pestana, N. Mardirossian, M. Head-Gordon, T. Head-Gordon, *Chem. Sci.* **2017**, *8*, 3554.
- [56] J. Liu, X. He, J. Z. H. Zhang, L.-W. Qi, *Chem. Sci.* **2018**, *9*, 2065.
- [57] K. Zhong, C.-C. Yu, M. Dodia, M. Bonn, Y. Nagata, T. Ohto, *Phys. Chem. Chem. Phys.* **2020**, *22*, 12785.
- [58] A. Priyadarsini, S. Dasari, B. S. Mallik, *J. Phys. Chem. A* **2020**, *124*, 6039.
- [59] K. Zhou, C. Qian, Y. Liu, *J. Phys. Chem. B* **2022**, *126*, 10471.
- [60] A. Bankura, V. Carnevale, M. L. Klein, *J. Chem. Phys.* **2013**, *138*, 014501.
- [61] Y. Ding, A. A. Hassanali, M. Parrinello, *Proc. Natl. Acad. Sci. USA* **2014**, *111*, 3310.
- [62] Y. Ding, *Comput. Theor. Chem.* **2019**, 1153, 25.
- [63] L. Zhou, J. Xu, L. Xu, X. Wu, *J. Chem. Phys.* **2019**, *150*, 124505.
- [64] T. T. Duignan, G. K. Schenter, J. L. Fulton, T. Huthwelker, M. Balasubramanian, M. Galib, M. D. Baer, J. Wilhelm, J. Hutter, M. Del Ben, X. S. Zhao, C. J. Mundy, *Phys. Chem. Chem. Phys.* **2020**, *22*, 10641.
- [65] X. Wang, D. Toroz, S. Kim, S. L. Clegg, G.-S. Park, D. Di Tommaso, *Phys. Chem. Chem. Phys.* **2020**, *22*, 16301.
- [66] M.-T. Nguyen, V.-A. Glezakou, J. Lonergan, B. Mc-Namara, P. D. Paviot, R. Rousseau, *J. Mol. Liq.* **2021**, *326*, 115262.
- [67] F. Tang, J. Xu, D. Y. Qiu, X. Wu, *Phys. Rev. B* **2021**, *104*, 035117.
- [68] S. Roy, M. Brehm, S. Sharma, F. Wu, D. S. Maltsev, P. Halstenberg, L. C. Gallington, S. M. Mahurin, S. Dai, A. S. Ivanov, C. J. Margulis, V. S. Bryantsev, *J. Phys. Chem. B* **2021**, *125*, 5971.
- [69] N. Holmberg, J.-C. Chen, A. S. Foster, K. Laasonen, *Phys. Chem. Chem. Phys.* **2014**, *16*, 17437.
- [70] K. Yue, B. Doherty, O. Acevedo, *J. Phys. Chem. B* **2022**, *126*, 3908.
- [71] D. Tolmachev, N. Lukasheva, R. Ramazanov, V. Nazarychev, N. Borzdun, I. Volgin, M. Andreeva, A. Glova, S. Melnikova, A. Dobrovskiy, S. A. Silber, S. Larin, R. Maglia de Souza, M. C. C. Ribeiro, S. Lyulin, M. Karttunen, *Int. J. Mol. Sci.* **2022**, *23*, 645.
- [72] S. Kishinaka, A. Morita, T. Ishiyama, *J. Chem. Phys.* **2019**, *150*, 044707.
- [73] R. Kronberg, K. Laasonen, *J. Phys. Chem. Lett.* **2021**, *12*, 10128.
- [74] R. Kronberg, K. Laasonen, *J. Phys. Chem. C* **2020**, *124*, 13706.
- [75] G. Cassone, H. Kruse, J. Sponer, *Phys. Chem. Chem. Phys.* **2019**, *21*, 8121.
- [76] A. Szabadi, R. Elfgen, R. Macchieraldo, F. L. Kearns, H. Lee Woodcock, B. Kirchner, C. Schröder, *J. Mol. Liq.* **2021**, *337*, 116521.
- [77] T. D. Kühne, T. A. Pascal, E. Kaxiras, Y. Jung, *J. Phys. Chem. Lett.* **2011**, *2*, 105.
- [78] N. V. Ryzhkov, O. Ledovich, L. Eggert, A. Bund, A. Paszuk, T. Hannappel, K. Klyukin, V. Alexandrov, E. V. Skorb, *ACS Appl. Nano Mater.* **2020**, *4*, 425.
- [79] T. Ogawa, T. Aonuma, T. Tamaki, H. Ohashi, H. Ushiyama, K. Yamashita, T. Yamaguchi, *Chem. Sci.* **2014**, *5*, 4878.
- [80] J. A. Elliott, S. J. Paddison, *Phys. Chem. Chem. Phys.* **2007**, *9*, 2602.
- [81] Y. Zhang, E. Yildirim, H. S. Antila, L. D. Valenzuela, M. Sammalkorpi, J. L. Lutkenhaus, *Soft Matter* **2015**, *11*, 7392.
- [82] R. Zhang, Y. Zhang, H. S. Antila, J. L. Lutkenhaus, M. Sammalkorpi, *J. Phys. Chem. B* **2017**, *121*, 322.
- [83] E. Yildirim, Y. Zhang, J. L. Lutkenhaus, M. Sammalkorpi, *ACS Macro Lett.* **2015**, *4*, 1017.
- [84] M. Khavani, P. Batys, S. M. Lalwani, C. I. Eneh, A. Leino, J. L. Lutkenhaus, M. Sammalkorpi, *Macromolecules* **2022**, *55*, 3140.
- [85] P. A. Sánchez, M. Vögele, J. Smiatek, B. Qiao, M. Sega, C. Holm, *Soft Matter* **2019**, *15*, 9437.
- [86] P. A. Sánchez, M. Vögele, J. Smiatek, B. Qiao, M. Sega, C. Holm, *Molecules* **2020**, *25*, 1848.
- [87] M. Vögele, C. Holm, J. Smiatek, *J. Chem. Phys.* **2015**, *143*, 243151.
- [88] M. J. Abraham, T. Murtola, R. Schulz, S. Páll, J. C. Smith, B. Hess, E. Lindahl, *SoftwareX* **2015**, *1–2*, 19.
- [89] W. L. Jorgensen, J. Tirado-Rives, *J. Am. Chem. Soc.* **1988**, *110*, 1657.
- [90] W. L. Jorgensen, J. Gao, *J. Phys. Chem.* **1986**, *90*, 2174.
- [91] W. L. Jorgensen, J. D. Madura, *Mol. Phys.* **1985**, *56*, 1381.
- [92] J. Åqvist, *J. Phys. Chem.* **1990**, *94*, 8021.
- [93] J. Chandrasekhar, D. C. Spellmeyer, W. L. Jorgensen, *J. Am. Chem. Soc.* **1984**, *106*, 903.
- [94] T. P. Lybrand, I. Ghosh, J. A. McCammon, *J. Am. Chem. Soc.* **1985**, *107*, 7793.
- [95] G. Bussi, D. Donadio, M. Parrinello, *J. Chem. Phys.* **2007**, *126*, 014101.
- [96] M. Parrinello, A. Rahman, *J. Appl. Phys.* **1981**, *52*, 7182.
- [97] U. Essmann, L. Perera, M. L. Berkowitz, T. Darden, H. Lee, L. G. Pedersen, *J. Chem. Phys.* **1995**, *103*, 8577.
- [98] B. Hess, H. Bekker, H. J. C. Berendsen, J. G. E. M. Fraaije, *J. Comput. Chem.* **1997**, *18*, 1463.
- [99] S. Miyamoto, P. A. Kollman, *J. Comput. Chem.* **1992**, *13*, 952.
- [100] J. Vandevondele, M. Krack, F. Mohamed, M. Parrinello, T. Chassaing, J. Hutter, *Comp. Phys. Commun.* **2005**, *167*, 103.

- [101] T. D. Kühne, M. Iannuzzi, M. Del Ben, V. V. Rybakin, P. Seewald, F. Stein, T. Laino, R. Z. Khaliullin, O. Schütt, F. Schiffmann, D. Golze, J. Wilhelm, S. Chulkov, M. H. Bani-Hashemian, V. Weber, U. Borštnik, M. Taillefumier, A. S. Jakobovits, A. Lazzaro, H. Abast, T. Müller, R. Schade, M. Guidon, S. Andermatt, N. Holmberg, G. K. Schenter, A. Hehn, A. Bussy, F. Belleflamme, G. Tabacchi, A. Glöb, M. Lass, I. Bethune, C. J. Mundy, C. Plessl, M. Watkins, J. VandeVondele, M. Krack, J. Hutter, *J. Chem. Phys.* **2020**, *152*, 194103.
- [102] J. P. Perdew, K. Burke, M. Ernzerhof, *Phys. Rev. Lett.* **1996**, *77*, 3865.
- [103] S. Grimme, J. Antony, S. Ehrlich, H. Krieg, *J. Chem. Phys.* **2010**, *132*, 154104.
- [104] S. Grimme, S. Ehrlich, L. Goerigk, *J. Comput. Chem.* **2011**, *32*, 1456.
- [105] J. VandeVondele, J. Hutter, *J. Chem. Phys.* **2007**, *127*, 114105.
- [106] S. Goedecker, M. Teter, *Phys. Rev. B* **1996**, *54*, 1703.
- [107] C. Hartwigsen, S. Goedecker, J. Hutter, *Phys. Rev. B* **1998**, *58*, 3641.
- [108] M. Krack, *Theor. Chem. Acc.* **2005**, *114*, 145.
- [109] J. VandeVondele, J. Hutter, *J. Chem. Phys.* **2003**, *118*, 4365.
- [110] R. H. Byrd, P. Lu, J. Nocedal, C. Zhu, *SIAM J. Sci. Comp.* **2006**, *16*, 1190.
- [111] J. VandeVondele, F. Mohamed, M. Krack, J. Hutter, M. Sprik, M. Parrinello, *J. Chem. Phys.* **2005**, *122*, 014515.
- [112] W. C. Swope, H. C. Andersen, P. H. Berens, K. R. Wilson, *J. Chem. Phys.* **1998**, *76*, 637.
- [113] W. Humphrey, A. Dalke, K. Schulten, *J. Mol. Graphics* **1996**, *14*, 33.
- [114] N. Michaud-Agrawal, E. J. Denning, T. B. Woolf, O. Beckstein, *J. Comput. Chem.* **2011**, *32*, 2319.
- [115] R. J. Gowers, M. Linke, J. Barnoud, T. J. E. Reddy, M. N. Melo, S. L. Seyler, J. Domański, D. L. Dotson, S. Buchoux, I. M. Kenney, O. Beckstein, MDAnalysis: A Python Package for the Rapid Analysis of Molecular Dynamics Simulations, in S. Benthall, S. Rostrup (Editors), *Proceedings of the 15th Python in Science Conference* **2016** pages 98–105.
- [116] R. D. Shannon, *Acta Crystallogr. Sect. A* **1976**, *32*, 751.
- [117] E. R. J. Nightingale, *J. Phys. Chem.* **1959**, *63*, 1381.
- [118] M. Galib, M. D. Baer, L. B. Skinner, C. J. Mundy, T. Huthwelker, G. K. Schenter, C. J. Benmore, N. Govind, J. L. Fulton, *J. Chem. Phys.* **2017**, *146*, 084504.
- [119] J. Mähler, I. Persson, *Inorg. Chem.* **2012**, *51*, 425.
- [120] R. Mancinelli, A. Botti, F. Bruni, M. A. Ricci, A. K. Soper, *J. Phys. Chem. B* **2007**, *111*, 13570.
- [121] A. Tongraar, J. T-Thienprasert, S. Rujirawat, S. Limpijumngong, *Phys. Chem. Chem. Phys.* **2010**, *12*, 10876.
- [122] L. X. Dang, G. K. Schenter, V.-A. Glezakou, J. L. Fulton, *J. Phys. Chem. B* **2006**, *110*, 23644.
- [123] D. T. Bowron, *J. Phys. Conf. Ser.* **2009**, *190*, 012022.
- [124] F. Sessa, P. D'Angelo, L. Guidoni, V. Migliorati, *J. Phys. Chem. B* **2015**, *119*, 15729.
- [125] P. D'Angelo, A. Di Nola, A. Filippini, N. V. Pavel, D. Roccatano, *J. Chem. Phys.* **1994**, *100*, 985.
- [126] Z. Jing, Y. Zhou, T. Yamaguchi, K. Yoshida, K. Ikeda, K. Ohara, G. Wang, *J. Phys. Chem. Lett.* **2023**, *14*, 6270.
- [127] P. D'Angelo, V. Migliorati, L. Guidoni, *Inorg. Chem.* **2010**, *49*, 4224.
- [128] M. J. Gillan, D. Alfè, A. Michaelides, *J. Chem. Phys.* **2016**, *144*, 130901.
- [129] Z. Jing, C. Liu, S. Y. Cheng, R. Qi, B. D. Walker, J.-P. Piquemal, P. Ren, *Annu. Rev. Biophys.* **2019**, *48*, 371.
- [130] K. Goloviznina, J. N. Canongia Lopes, M. Costa Gomes, A. A. H. Pádua, *J. Chem. Theory Comput.* **2019**, *15*, 5858.
- [131] K. Goloviznina, Z. Gong, M. F. Costa Gomes, A. A. H. Pádua, *J. Chem. Theory Comput.* **2021**, *17*, 1606.
- [132] K. Goloviznina, Z. Gong, A. A. H. Padua, *WIREs Comput. Mol. Sci.* **2022**, *12*, e1572.
- [133] R. Maglia de Souza, M. Karttunen, M. C. C. Ribeiro, *J. Chem. Inf. Model.* **2021**, *61*, 5938.
- [134] A. Szabadi, R. Elfgen, R. Macchieraldo, F. L. Kearns, H. Lee Woodcock, B. Kirchner, C. Schröder, *J. Mol. Liq.* **2021**, *337*, 116521.

Manuscript received: March 5, 2024
Revised manuscript received: May 2, 2024
Accepted manuscript online: May 7, 2024
Version of record online: June 20, 2024